

Process dependence of AlAs/GaAs superlattice mixing induced by silicon implantation

S. A. Schwarz, T. Venkatesan, D. M. Hwang, H. W. Yoon, R. Bhat, and Y. Arakawa

Citation: [Applied Physics Letters](#) **50**, 281 (1987); doi: 10.1063/1.98225

View online: <http://dx.doi.org/10.1063/1.98225>

View Table of Contents: <http://scitation.aip.org/content/aip/journal/apl/50/5?ver=pdfcov>

Published by the [AIP Publishing](#)

Articles you may be interested in

[Oxidation induced AlAs/GaAs superlattice disordering](#)

Appl. Phys. Lett. **60**, 1235 (1992); 10.1063/1.107416

[MeV oxygen ion implantation induced compositional intermixing in AlAs/GaAs superlattices](#)

Appl. Phys. Lett. **57**, 896 (1990); 10.1063/1.103397

[Kinetics of silicon-induced mixing of AlAs-GaAs superlattices](#)

Appl. Phys. Lett. **50**, 1823 (1987); 10.1063/1.97709

[Dose-dependent mixing of AlAs-GaAs superlattices by Si ion implantation](#)

Appl. Phys. Lett. **49**, 701 (1986); 10.1063/1.97635

[Disorder of an AlAs-GaAs superlattice by silicon implantation](#)

Appl. Phys. Lett. **40**, 904 (1982); 10.1063/1.92942

The image shows the cover of the journal Applied Physics Reviews. It features a white background with a blue and orange design. The title 'AIP Applied Physics Reviews' is at the top. Below it is a diagram of a superlattice structure. The text 'april 2015' is at the bottom left.

NEW Special Topic Sections

NOW ONLINE
Lithium Niobate Properties and Applications:
Reviews of Emerging Trends

AIP Applied Physics Reviews

Process dependence of AlAs/GaAs superlattice mixing induced by silicon implantation

S. A. Schwarz, T. Venkatesan, D. M. Hwang, H. W. Yoon, and R. Bhat
Bell Communications Research, Inc., Red Bank, New Jersey 07701-7020

Y. Arakawa
University of Tokyo, Roppongi, Minato-Ku 106, Japan

(Received 29 September 1986; accepted for publication 2 December 1986)

Silicon implantation induced mixing of a 400-Å period AlAs/GaAs superlattice grown by organometallic chemical vapor deposition is examined using secondary ion mass spectrometry and transmission electron microscopy. The depth dependence of Al and Si diffusion for a 180-kV $3 \times 10^{15} \text{ cm}^{-2} \text{ Si}^+$ implant is measured as a function of implantation temperature, annealing temperature, and annealing time. The room-temperature implanted sample exhibits a near-surface mixing inhibition following anneal. No mixing inhibition is observed in samples implanted at higher temperatures. Si segregates rapidly into the GaAs layers during the anneal. Si diffusion is inhibited near the peak of the implant. Mixing depths and defect distributions are strongly dependent on the processing conditions employed. The results are consistent with a divacancy model for Al diffusion.

Superlattice mixing and its potential application in optoelectronic devices are the subjects of several recent papers.¹⁻⁸ Recently, we examined the dose dependence of AlAs/GaAs superlattice mixing induced by Si implantation and subsequent anneal.^{9,10} In this letter, we extend this work by observing the effect of implantation temperature, annealing temperature, and annealing time on the mixing induced by Si implantation. Al and Si diffusion is monitored by secondary ion mass spectrometry (SIMS). Defect distributions are examined with transmission electron microscopy (TEM). Mixing behavior is found to be strongly process dependent.

A 40-period superlattice grown by organometallic chemical vapor deposition (OMCVD) with layer thicknesses of 150 Å AlAs and 250 Å GaAs was examined. Samples were implanted at room temperature, 150, 250, and 350 °C with a $3 \times 10^{15} \text{ cm}^{-2}$ 180 kV $^{28}\text{Si}^+$ implant. Anneals were performed at 700, 750, 800, and 850 °C with a silicon nitride cap in a hydrogen ambient. The nitride was then plasma etched so as not to affect the top layer of the superlattice. Al stoichiometry was profiled by an Atomika 3000-30 SIMS instrument with a 6-kV normally incident O_2^+ beam. The Si implants were profiled with a 15-kV beam. TEM bright and dark field micrographs were obtained in a JEOL 2000FX using the (002) diffraction configuration for layer delineation and the (111) diffraction configuration for defect enhancement. The experimental conditions are identical to those described in Refs. 9 and 10.

The SIMS profiles of Al and Si in the 350 °C implant before and after a 3-h 850 °C anneal are shown in Fig. 1. In the as-implanted sample, the Al oscillations decrease near the surface over a distance corresponding roughly to the projected range ($\sim 1800 \text{ Å}$). In the annealed sample, the surface region is well mixed with oscillations gradually reappearing in the lower region of the superlattice. (The as-implanted Si profile displays oscillations which are due to differing SIMS sensitivities in the AlAs and GaAs layers.⁹) The lack of diffusion near the surface and the sharp drop in Si concentration deep in the superlattice are typical features

of all the annealed Si profiles. A small dopant spike is also observed in the figure at the growth interface. The TEM (002) bright field micrographs for the samples examined in Fig. 1 are shown in Fig. 2. A high density of dislocation loops near the as-implanted sample are annealed out leaving a small number of large diameter ($\sim 500 \text{ Å}$) loops in a good quality mixed region.

The results of Figs. 1 and 2 are in marked contrast to the room-temperature implant examined in Refs. 9 and 10. The corresponding room-temperature implant exhibited a lack of Al mixing near the peak of the implant. This unmixed region displayed a large density of small ($< 80 \text{ Å}$) dislocation loops. The total depth of mixing was significantly less than observed in Fig. 1. The as-implanted room-temperature sample showed a high density of stacking faults and microtwins near the surface. The behavior of the Si profiles, however, was similar to that observed here with an inhibition of Si diffusion near the implant peak.

We have previously shown^{9,10} that the Al peak-to-valley ratios extracted from data such as in Fig. 1 can, to first order, be converted to Al diffusion lengths $2(Dt)^{1/2}$. The procedure assumes that the superlattice may be approximated as the sum of a periodic array of gaussians with half-widths proportional to the diffusion length. Al diffusion lengths extracted in this manner are shown in Fig. 3. The three boxes in the figure correspond, from top to bottom, to implant temperatures of 150, 250, and 350 °C, respectively. The 150 °C samples were annealed at 850 °C for times of 10 min, 20 min, 1.5 h, and 3 h. The 250 °C samples were annealed for 3 h at temperatures of 700, 750, and 800 °C. The 350 °C sample was annealed at 850 °C for 3 h and corresponds to the data of Fig. 1. The time-dependence data at the top of the figure shows that mixing occurs initially in the damaged near-surface region and extends at longer times deep into the superlattice. Al mixing and Si diffusion extend to significantly greater depths following anneal as the implant temperature increases, despite the fact that no significant diffusion is observed in the as-implanted samples.

The Si diffusion profiles from the time-dependence

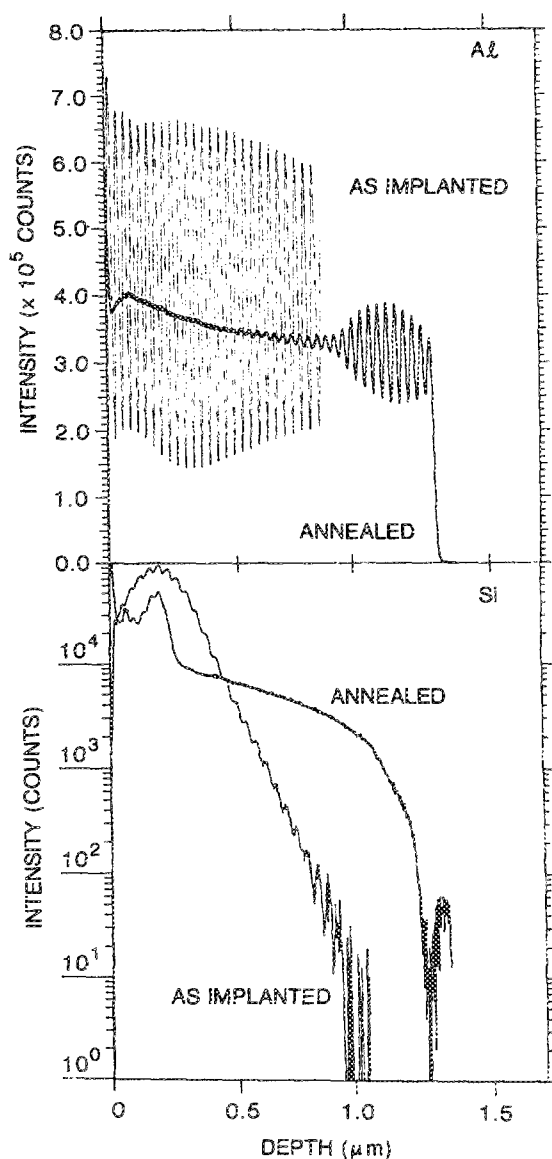


FIG. 1. 350 °C, 180 kV, $3 \times 10^{15} \text{ cm}^{-2} \text{ Si}^+$ implant is examined with SIMS before and after a 3-h 850 °C anneal. The top linear plot shows the Al oscillations; the bottom log plot shows corresponding Si depth profiles.

study at 150 °C are plotted on a linear scale in Fig. 4. The profiles are shifted on the vertical axis for clarity with the shortest annealing time at the top. The Si segregation is observed to occur quite rapidly in comparison with Al intermixing. At 20 min the Si oscillations are already beginning to decrease due to diffusion near the peak of the implant while somewhat beyond the peak, additional oscillations have appeared. At longer times, Si diffuses very gradually well after complete Al intermixing has occurred.

While no definitive explanation of these results is yet possible, the following interpretation is consistent with the observations to date: Al mixing appears to depend both on the mechanism of Si pair diffusion and on the concentration of vacancies which support diffusion of Si and Al. The sharp dropoff of the Si concentration profile is a natural result of the Si pair diffusion model in which rapid pair diffusion is most likely to occur at high Si concentrations.¹¹ The dropoff occurs in all samples at a concentration of roughly 10^{18} cm^{-3} at the depth where superlattice mixing abruptly ceases.^{7,9} The gradual decrease of the Al diffusion length in the 350 °C sample probably results from the fact that, at depths greater than $0.7 \mu\text{m}$, the net time during which the Si concentration is greater than 10^{18} cm^{-3} is small. While Si pair diffusion does not necessarily increase vacancy concentrations, it greatly increases the mobility of both anion (As) and cation (Ga, Al) vacancies. In particular, by alternately moving anion and cation vacancies, divacancies can be created with high probability. The activation energy for Al motion through a divacancy is clearly reduced since Al atoms can jump through an As vacancy into the neighboring cation vacancy. Van Vechten¹² has shown that a divacancy mechanism may be important in Zn-induced superlattice mixing. In that model, the Zn interstitial interacts with the divacancy to lower the activation energy for an Al jump. For Si the primary effect may be the increased generation rate of divacancies.

The slow diffusion of Si near the implant peak is more difficult to interpret. At Si concentrations well above 10^{20} cm^{-3} , Burnham *et al.*¹³ have shown that a high quality $(\text{Si}_2)_x (\text{GaAs})_{1-x}$ alloy can form. A 23-Å alloy layer was

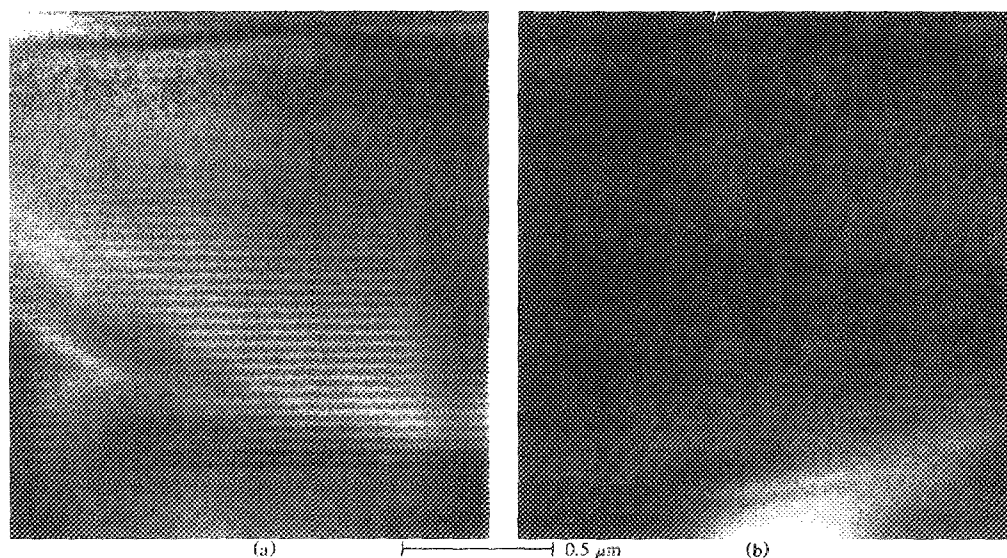


FIG. 2. TEM (002) bright field micrographs of the (a) unannealed and (b) annealed samples examined Fig. 1.

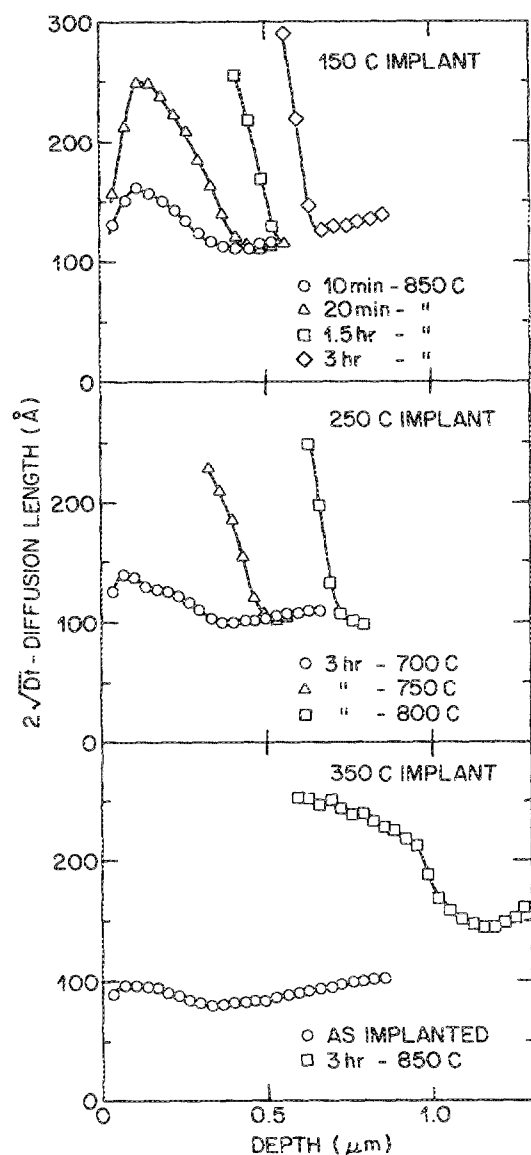


FIG. 3. Al diffusion lengths vs depth extracted from SIMS data. The upper box shows the time dependence of mixing for the 150 °C implant. The center box shows the annealing temperature dependence for the 250 °C implant. The lower box shows the pre- and post-annealed 350 °C implant and corresponds to the data at the top of Fig. 1.

formed at a growth temperature over 800 °C. Diffusion in the alloy may be somewhat inhibited. It also is possible that vacancies are consumed near the implant peak by the high concentration of Si interstitials following implantation. In the room-temperature sample, a high concentration of defect loops in the implant peak region^{9,11} may have gettered out the available point defects. Remnant defect loops might also getter Al and Si. Bhattacharya *et al.*¹⁴ have observed that little Si precipitation occurs in GaAs under conditions similar to those employed here. The sloping Al profile in Fig. 1 suggests that the flux of Al into the implant peak region is greater than the outgoing flux. Al diffusion therefore seems to be somewhat inhibited in this region also, as was certainly observed at room temperature where Al mixing was inhibited. The rapid Si segregation into the GaAs layers may be due in part to preferential damage of these layers,¹⁰ as observed in the TEM(111) micrographs. The implant-temperature

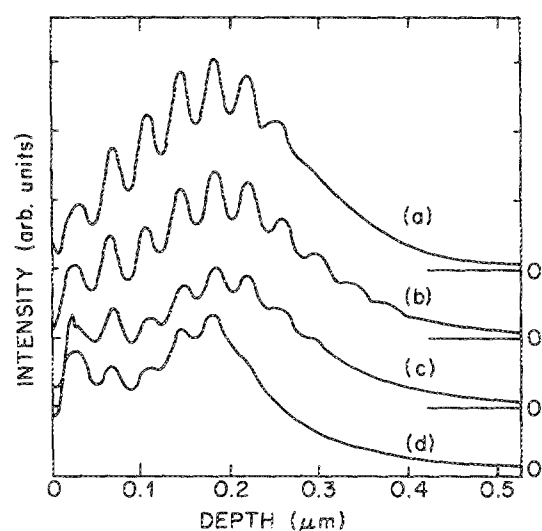


FIG. 4. Linear plot of the Si profiles for the 150 °C implant for annealing times of (a) 10 min, (b) 20 min, (c) 1.5 h, and (d) 3 h at 850 °C. The plots are shifted on the vertical axis and the horizontal scale is expanded for clarity.

dependence seems to indicate higher vacancy concentrations in the samples implanted at elevated temperatures, resulting in complete mixing near the surface and in enhanced Si diffusion and hence deeper mixing.

In summary, the depth dependence of Al and Si diffusion and segregation has been monitored by SIMS. The crystalline quality and nature of the defects have been examined with TEM. Elevated implant temperatures are found to induce complete mixing near the surface. The results are interpreted in terms of a divacancy model. The observed variations of mixing behavior with implant temperature, annealing temperature, and annealing time should prove useful in the selection of appropriate experimental parameters for particular device applications.

¹N. Holonyak, Jr., W. D. Laidig, M. D. Camras, J. J. Coleman, and P. D. Dapkus, *Appl. Phys. Lett.* **39**, 102 (1981).

²J. J. Coleman, P. D. Dapkus, C. G. Kirkpatrick, M. D. Camras, and N. Holonyak, Jr., *Appl. Phys. Lett.* **40**, 904 (1982).

³P. Gavrilovic, D. G. Deppe, K. Meehan, N. Holonyak, Jr., J. J. Coleman, and R. D. Burnham, *Appl. Phys. Lett.* **47**, 130 (1985).

⁴J. W. Lee and W. D. Laidig, *J. Electron. Mater.* **13**, 147 (1984).

⁵M. Kawabe, N. Matsuura, N. Shimizu, F. Hasegawa, and V. Nannichi, *Jpn. J. Appl. Phys.* **23**, L623 (1984).

⁶Y. Hirayama, Y. Suzuki, S. Tarucha, and H. Okamoto, *Jpn. J. Appl. Phys.* **24**, L516 (1985).

⁷J. Kobayashi, M. Nakajima, Y. Bamba, T. Fukunaga, K. Matsui, K. Ishida, H. Nakashima, and K. Ishida, *Jpn. J. Appl. Phys.* **25**, L385 (1986).

⁸J. Ralston, G. W. Wicks, L. F. Eastman, B. C. DeCooman, and C. B. Carter, *J. Appl. Phys.* **59**, 120 (1986).

⁹S. A. Schwarz, T. Venkatesan, R. Bhat, M. Koza, H. W. Yoon, Y. Arakawa, and P. Mei, 1985 MRS Symp. Layered Structures and Epitaxy (to be published by Materials Research Society, Pittsburgh, PA).

¹⁰T. Venkatesan, S. A. Schwarz, D. M. Hwang, R. Bhat, M. Koza, H. W. Yoon, P. Mei, Y. Arakawa, and A. Yariv, *Appl. Phys. Lett.* **49**, 701 (1986).

¹¹M. E. Greiner and J. F. Gibbons, *J. Appl. Phys.* **57**, 5181 (1985).

¹²J. A. Van Vechten, *J. Appl. Phys.* **53**, 708 (1982).

¹³R. D. Burnham, N. Holonyak, Jr., K. C. Hsieh, R. W. Kalisky, D. W. Nam, R. L. Thornton, and T. L. Paoli, *Appl. Phys. Lett.* **48**, 800 (1986).

¹⁴R. S. Bhattacharya, A. K. Rai, Y. K. Yeo, P. P. Pronko, S. C. Ling, S. R. Wilson, and Y. S. Park, *J. Appl. Phys.* **54**, 2329 (1983).